

# A nested double pseudoknot is required for self-cleavage activity of both the genomic and antigenomic hepatitis delta virus ribozymes

TIMOTHY S. WADKINS,<sup>1</sup> ANNE T. PERROTTA,<sup>1</sup> ADRIAN R. FERRÉ-D'AMARÉ,<sup>2</sup>  
JENNIFER A. DOUDNA,<sup>2,3</sup> and MICHAEL D. BEEN<sup>1</sup>

<sup>1</sup>Department of Biochemistry, Duke University Medical Center, Durham, North Carolina 27710, USA

<sup>2</sup>Department of Molecular Biophysics and Biochemistry, Yale University, New Haven, Connecticut 06520, USA

<sup>3</sup>Howard Hughes Medical Institute, Yale University, New Haven, Connecticut 06520, USA

## ABSTRACT

The crystal structure of a genomic hepatitis delta virus (HDV) ribozyme 3' cleavage product predicts the existence of a 2 bp duplex, P1.1, that had not been previously identified in the HDV ribozymes. P1.1 consists of two canonical C-G base pairs stacked beneath the G•U wobble pair at the cleavage site and would appear to pull together critical structural elements of the ribozyme. P1.1 is the second stem of a second pseudoknot in the ribozyme, making the overall fold of the ribozyme a nested double pseudoknot. Sequence comparison suggests the potential for P1.1 and a similar fold in the antigenomic ribozyme. In this study, the base pairing requirements of P1.1 for cleavage activity were tested in both the genomic and antigenomic HDV ribozymes by mutagenesis. In both sequences, cleavage activity was severely reduced when mismatches were introduced into P1.1, but restored when alternative base pairing combinations were incorporated. Thus, P1.1 is an essential structural element required for cleavage of both the genomic and antigenomic HDV ribozymes and the model for the antigenomic ribozyme secondary structure should also be modified to include P1.1.

**Keywords:** catalytic RNA; hepatitis delta virus; RNA structure; self-cleaving RNA

## INTRODUCTION

Hepatitis delta virus (HDV) is a human pathogen that propagates itself as a satellite of the hepatitis B virus (Rizzetto, 1983; Lai, 1995). This circular, single-stranded RNA virus is the only known human pathogen that utilizes ribozymes as a component of its life cycle (Lai, 1995). The HDV genome, which is approximately 1.7 kb in length, is believed to form a rod-like structure because of extensive self-complementarity between the two halves of the molecule (Kos et al., 1986; Wang et al., 1986). The genome contains a self-cleaving ribozyme sequence (Kuo et al., 1988; Sharmeen et al., 1988; Wu et al., 1989) that can function in vitro at a minimal size of 85 nt (Perrotta & Been, 1990, 1991). Similarly, the antigenomic strand, formed intracellularly during replication of the genomic strand, also contains a self-cleaving sequence (Kuo et al., 1988; Sharmeen et al., 1988). Because of the high degree of comple-

mentarity of the HDV genome, these ribozymes have very similar, though not completely identical, sequences and are believed to form related secondary structures (Perrotta & Been, 1991). The ribozyme sequences are essential for the replication of HDV and appear to process multimers formed from rolling circle replication to monomeric form (MacNaughton et al., 1993; Jeng et al., 1996).

The HDV ribozymes are often grouped with the other small self-cleaving RNAs: the hammerhead, hairpin, and *Neurospora* VS ribozymes (Symons, 1992). All of these ribozymes generate cleavage products with a 2',3'-cyclic phosphate group and a 5' OH group (Kuo et al., 1988; Sharmeen et al., 1988; Wu et al., 1989). There are four distinct secondary structural motifs associated with these four classes of small ribozymes, but, for several years, the only crystal structure was of the hammerhead (Pley et al., 1994; Scott et al., 1995). A high-resolution structure of a genomic hepatitis delta virus ribozyme 3' cleavage product has recently been solved (Ferré-D'Amaré et al., 1998). Whereas the proposed secondary structure (Perrotta & Been, 1991) contained a single pseudoknot (Pleij et al., 1985; Pleij,

Reprint requests to: Michael D. Been, Department of Biochemistry, Duke University Medical Center, Durham, North Carolina 27710, USA; e-mail: been@biochem.duke.edu.

1990) defined by P1 and P2 (Fig. 1A), the crystal structure revealed a more complicated fold containing an additional pseudoknot (Fig. 1B) formed by P3 and a short helix, P1.1. P1.1 contains only 2 bp: C21–G39 and C22–G38. The combination of P1 and P1.1 defines yet a third, although overlapping, pseudoknot in which the cleavage site would appear to be defined, in part, by a contortion in the path of the 5' entering strand at the stacking interface of the two helices. Locally, P1.1 forms the bottom of a potential active-site pocket and stacks below the G1•U37 wobble pair that defines

the cleavage site (Fig. 2). In the overall structure, P1.1 appears to tie together several key elements of the ribozyme: the P1 substrate-bearing helix, the stacked P2 and P3 helices, and P4 with its associated J4/2 region (Ferré-D'Amaré et al., 1998).

Functional evidence for P1.1 in the HDV ribozyme cleavage reaction would provide a persuasive supplement to the structural data. In the HDV ribozymes, a single nucleotide 5' to the cleavage site is sufficient for cleavage (Perrotta & Been, 1990, 1992). Thus, it has been convenient to use the 3' product for a number of structural studies of the RNA in solution (Rosenstein & Been, 1991, 1996; Kumar et al., 1994). Likewise, the HDV ribozyme crystal structure is of the postcleavage 3' product RNA. Although the sequence requirements 5' to the cleavage site are minimal, the nucleotide 5' to the cleavage site is obviously a critical and essential component of the self-cleaving molecule. Some secondary structural models for the genomic HDV ribozyme precursor have the nucleotide 5' to the cleavage site (U-1) base paired to G38 (Kawakami et al., 1993; Kumar et al., 1993, 1994; Thill et al., 1993; Tanner et al., 1994). Although a G38•U-1 wobble would be incompatible with canonical pairing of G38 to C22 (Fig. 1), an argument could be made that the C22–G38 base pair of P1.1 represents an alternative pairing arrangement present only in the product. Additionally, to solve the crystal structure, a high affinity binding site for the U1A protein RNA-binding domain (U1A-RBD) was engineered into the P4 duplex of the ribozyme, and the ribozyme/U1A-RBD ribonucleoprotein complex was crystallized. Having this domain and protein bound to the ribozyme, while not preventing self-cleavage activity in *in vitro* assays (Ferré-D'Amaré et al., 1998), raises issues about effects these elements might have during crystallization. Finally, given the sequence similarity between the genomic and antigenomic HDV ribozymes, especially in that the L3 and J1/4 regions in the antigenomic sequence are avail-

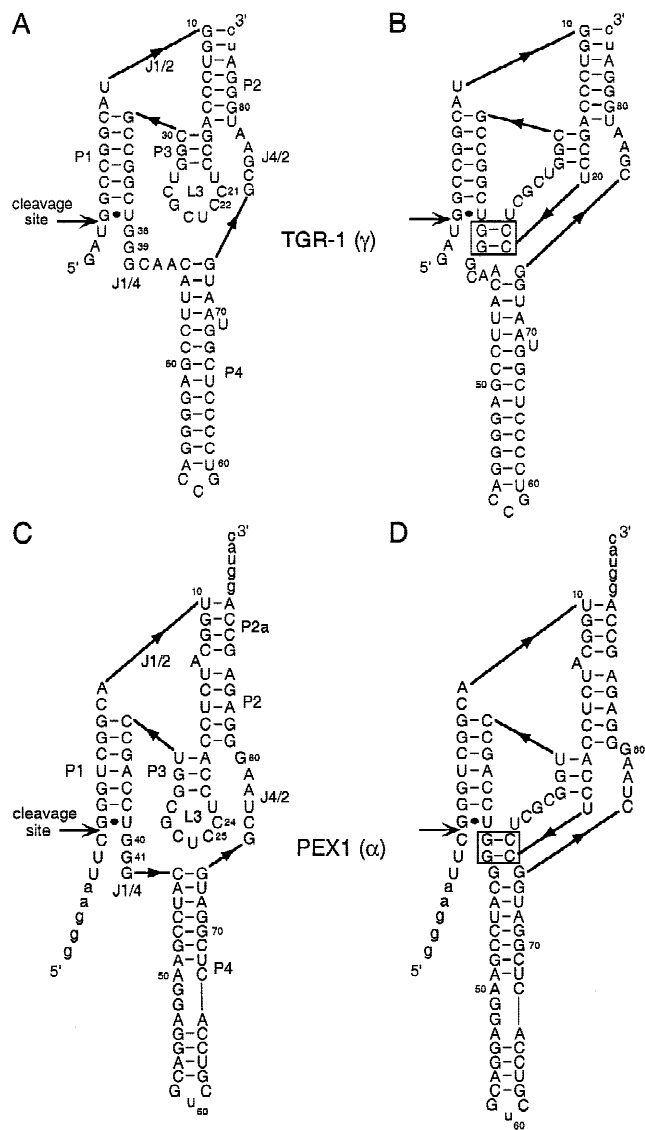


**FIGURE 1.** Secondary structures of the TGR-1 (genomic) and the PEX1 (antigenomic) HDV ribozyme sequences. **A** and **C**: Pseudoknot structures of the genomic and antigenomic ribozymes, respectively. **B**: Double pseudoknot structure of the genomic ribozyme. **D**: Proposed double pseudoknot structure of the antigenomic ribozyme. The P1.1 duplex is boxed in **B** and **D**. For simplicity, labels for paired and joining elements have been omitted in **B** and **D**. The entire sequence of each precursor is shown, the cleavage site is indicated, and lower case letters at the 5' and 3' ends are non-HDV sequences contributed by the vector.

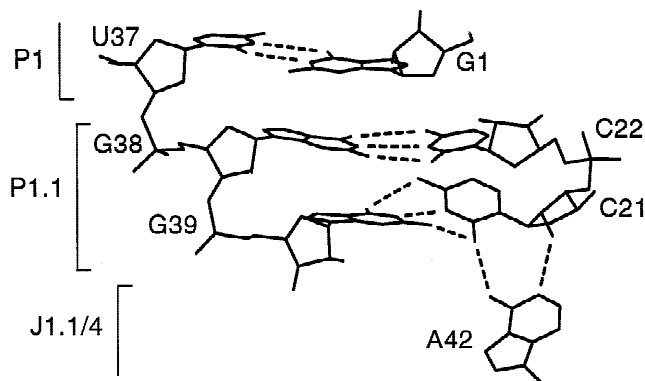


**FIGURE 2.** The P1.1 duplex region of the genomic ribozyme shown stacked below the cleavage site G•U pair (Ferré-D'Amaré et al., 1998).

able for the equivalent of a P1.1 pairing (Fig. 1C), it is reasonable to hypothesize a requirement for P1.1 in the antigenomic ribozyme as well (Fig. 1D).

To test the functional contribution of P1.1 to cleavage activity, mutations and potential compensatory changes were generated in both the genomic and antigenomic ribozymes. Although it was known that mutations at any of the 4 nt comprising P1.1 caused severe effects on cleavage activity (Tanner et al., 1994; Perrotta & Been, 1996), the base pairing interactions that form P1.1 had never been tested. The results support the prediction that P1.1 is an important feature of both ribozymes and is required for full activity.

## RESULTS

### Properties of the unmodified genomic and antigenomic precursor sequences

The wild-type genomic ribozyme used in this study was TGR-1 (Wadkins & Been, 1997). Under standard reaction conditions for this ribozyme (37 °C, 10 mM Mg<sup>2+</sup>, pH 8.0), TGR-1 cleaved with a first-order rate constant of 26 min<sup>-1</sup> (Table 1). PEX1 (Perrotta & Been, 1998) was used as the antigenomic ribozyme starting sequence. Conditions for PEX1 cleavage were essentially the same as for the genomic ribozyme except that 0.5 mM spermidine was included in the preincubation

**TABLE 1.** Genomic P1.1 mutant ribozymes.

Ribozyme	<i>k</i> (min <sup>-1</sup> ) <sup>a</sup>	EP (%) <sup>b</sup>	<i>k</i> <sub>relative</sub> <sup>c</sup>
TGR-1 (wt)	26 (±3)	69 (±1)	1
+ 5M urea	10 (±1)	74 (±2)	
γC21g	0.04 (±0.02)	6 (±1)	1.5 × 10 <sup>-3</sup>
+ 5M urea	0.06 (±0.02)	6.7 (±0.5)	
γG39c	0.0066 (±0.0007)	99 (±7)	2.5 × 10 <sup>-4</sup>
+ 5M urea	0.012 (±0.003)	26 (±4)	
γC21g:G39c	0.31 (±0.01)	81 (±1)	1.2 × 10 <sup>-2</sup>
+ 5M urea	0.066 (±0.003)	80 (±1)	
γC22g	0.014 (±0.001)	59 (±3)	5.4 × 10 <sup>-4</sup>
+ 5M urea	<sup>d</sup>	4 (±1)	
γG38c	0.028 (±0.001)	85 (±1)	1.1 × 10 <sup>-3</sup>
+ 5M urea	0.029 (±0.001)	85 (±1)	
γC22g:G38c	0.53 (±0.02)	73 (±1)	2.0 × 10 <sup>-2</sup>
+ 5M urea	0.04 (±0.01)	53 (±5)	
γC22u	1.4 (±0.1)	79 (±1)	5.4 × 10 <sup>-2</sup>
+ 5M urea	0.082 (±0.009)	72 (±3)	
γG38a	0.0063 (±0.0006)	89 (±7)	2.4 × 10 <sup>-4</sup>
+ 5M urea	0.010 (±0.003)	35 (±7)	
γC22u:G38a	4.4 (±0.3)	51 (±1)	1.7 × 10 <sup>-1</sup>
+ 5M urea	0.46 (±0.05)	49 (±2)	

<sup>a</sup>Cleavage in 10 mM Mg<sup>2+</sup> at 37 °C. Averaged first order rate constant and standard deviation.

<sup>b</sup>EP: end point or extent of cleavage.

<sup>c</sup>Relative rate (*k*<sub>mutant</sub>/*k*<sub>wt</sub>).

<sup>d</sup>Because of the low endpoint of reaction of this mutant in 5 M urea, a cleavage rate was not calculated.

and reaction. This ribozyme cleaved with a first-order rate constant of 31 min<sup>-1</sup> (Table 2). For TGR-1, the base pairing in P1.1 is C21 with G39, and C22 with G38 (Fig. 1B). In PEX1, the predicted base pairing in P1.1 would be C24 with G41, and C25 with G40 (Fig. 1D). For the remainder of this article, the numbering of nucleotides in the genomic constructs will be denoted with a gamma (γ) and in the antigenomic constructs with an alpha (α).

### The bottom base pair of P1.1

Three mutants were created to test the γC21–G39 base pair in the genomic ribozyme. To introduce mismatches, two single mutants, γC21g and γG39c, were made. The former mutant generated a G•G mismatch and the latter introduced a C•C mismatch into the P1.1 duplex (Fig. 3C). Additionally, the double mutant, γC21g:G39c, was made to restore the potential for base pairing (Fig. 3C). As an initial screen for cleavage activity of the mutants, <sup>32</sup>P-labeled precursor RNAs were allowed to self-cleave for 1 min in the presence of 10 mM Mg<sup>2+</sup>. These samples, along with controls incubated in the absence of Mg<sup>2+</sup>, were fractionated by electrophoresis on a polyacrylamide gel under denaturing conditions. Under these conditions, the wild-type sequence (TGR-1) cleaved to 77% (Fig. 4A). Of the three mutants created to test this base pair, only the γC21g:G39c double mutant showed a significant product band (23% cleaved). The two mutants that contained a mismatch cleaved to less than 1%. Effects of the mutations were examined in more detail by following the complete kinetics of the reaction for each variant. The rate constant for cleavage of γC21g was down 650-fold and γG39c was down 3,900-fold (Table 1). However, when both mutations were introduced into the same precursor (γC21g:G39c), activity was only reduced 84-fold. These data provided

**TABLE 2.** Antigenomic P1.1 mutant ribozymes.

Ribozyme	<i>k</i> (min <sup>-1</sup> ) <sup>a</sup>	EP (%) <sup>b</sup>	<i>k</i> <sub>relative</sub> <sup>c</sup>
PEX1 (wt)	31 (±1)	77 (±1)	1
αC24g	0.0013 (±0.0001)	100 <sup>d</sup>	4.2 × 10 <sup>-5</sup>
αG41c	0.058 (±0.001)	81 (±1)	1.9 × 10 <sup>-3</sup>
αC24g:G41c	40 (±2)	86 (±1)	1.3
αC25g	0.0054 (±0.0002)	100 <sup>d</sup>	1.7 × 10 <sup>-4</sup>
αG40c	0.029 (±0.003)	82 (±3)	9.4 × 10 <sup>-4</sup>
αC25g:G40c	4.6 (±0.7)	71 (±5)	1.5 × 10 <sup>-1</sup>
αC25u	0.37 (±0.03)	92 (±3)	1.2 × 10 <sup>-2</sup>
αG40a	0.019 (±0.002)	81 (±4)	6.1 × 10 <sup>-4</sup>
αC25u:G40a	20 (±1)	83 (±1)	6.5 × 10 <sup>-1</sup>

<sup>a</sup>Cleavage in 10 mM Mg<sup>2+</sup> at 37 °C. Averaged first order rate constant and standard deviation.

<sup>b</sup>EP: end point or extent of cleavage.

<sup>c</sup>Relative rate (*k*<sub>mutant</sub>/*k*<sub>wt</sub>).

<sup>d</sup>These reactions were still linear after 2 h; therefore, their endpoints were set at 100%.

Genomic Mutants			wild-type P1.1	Antigenomic Mutants				
<b>A</b>	$\gamma$ C22g	$\gamma$ G38c	$\gamma$ C22g: $\gamma$ G38c	$5'$ $3'$ $k_{relative}$	<b>D</b>	$\alpha$ C25g	$\alpha$ G40c	$\alpha$ C25g: $\alpha$ G40c
	G g	c C	c - g			G g	c C	c - g
	G-C	G-C	G-C			G-C	G-C	G-C
	$5.4 \times 10^{-4}$	$1.1 \times 10^{-3}$	$2.0 \times 10^{-2}$			$1.7 \times 10^{-4}$	$9.4 \times 10^{-4}$	$1.5 \times 10^{-1}$
<b>B</b>	$\gamma$ C22u	$\gamma$ G38a	$\gamma$ C22u: $\gamma$ G38a		<b>E</b>	$\alpha$ C25u	$\alpha$ G40a	$\alpha$ C25u: $\alpha$ G40a
	G u	a C	a - u			G u	a C	a - u
	G-C	G-C	G-C		G-C	G-C	G-C	
	$5.4 \times 10^{-2}$	$2.4 \times 10^{-4}$	$1.7 \times 10^{-1}$		$1.2 \times 10^{-2}$	$6.1 \times 10^{-4}$	$6.5 \times 10^{-1}$	
<b>C</b>	$\gamma$ C21g	$\gamma$ G39c	$\gamma$ C21g: $\gamma$ G39c	<b>F</b>	$\alpha$ C24g	$\alpha$ G41c	$\alpha$ C24g: $\alpha$ G41c	
	G-C	G-C	G-C		G-C	G-C	G-C	
	G g	c C	c - g		G g	c C	c - g	
	$1.5 \times 10^{-3}$	$2.5 \times 10^{-4}$	$1.2 \times 10^{-2}$		$4.2 \times 10^{-5}$	$1.9 \times 10^{-3}$	1.3	

**FIGURE 3.** Mutations in the P1.1 duplex. The wild-type P1.1 duplex (center) and specific sets of P1.1 mutant duplexes (A–F) made in this study. A–C: Genomic mutants. D–F: Antigenomic mutants. Names of the mutant ribozyme sequences are shown above each duplex. The mutated bases are indicated with lowercase letters. The relative activity ( $k_{relative}$ ; taken from tables 1 and 2) is shown below each construct.

evidence that base pairing at this position in the P1.1 duplex is essential for self-cleavage activity of the genomic ribozyme. Flipping the base pair, however, did reduce activity by about two orders of magnitude.

The corresponding potential base pair in the antigenomic ribozyme,  $\alpha$ C24–G41, was also tested. Three antigenomic mutants were made: two single mutants,  $\alpha$ C24g (G•G mismatch) and  $\alpha$ G41c (C•C mismatch),

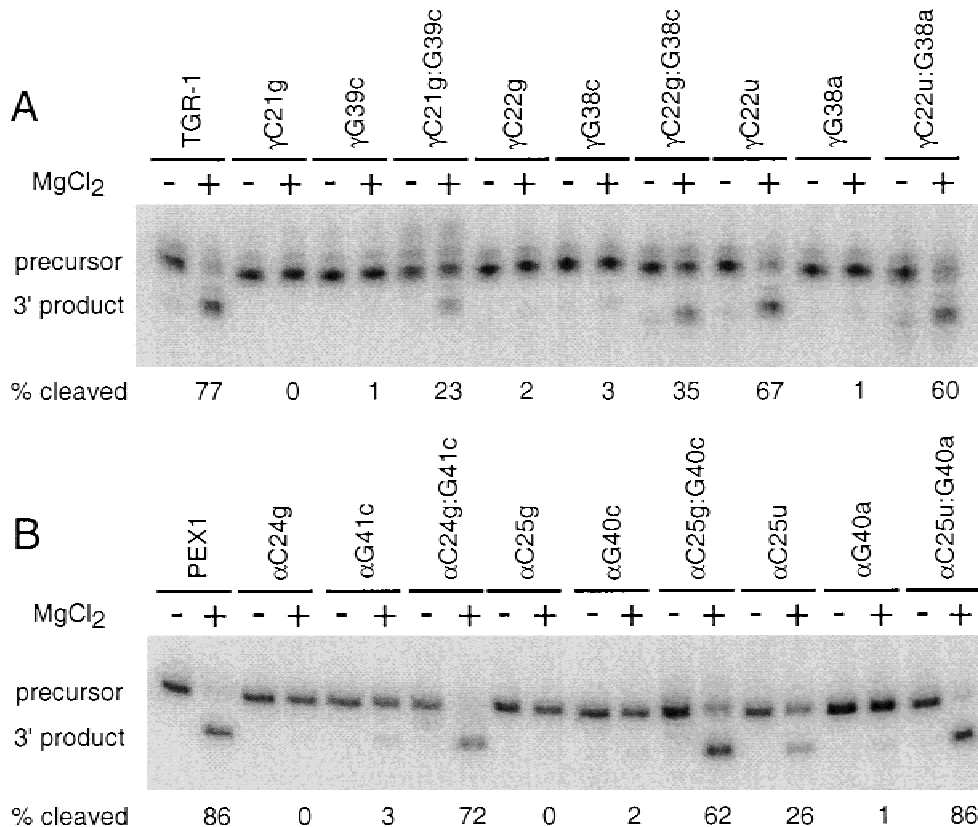


**FIGURE 4.** Cleavage of precursor RNAs. **A:** TGR-1 and mutants. **B:** PEX1 and mutants. For each RNA, a no Mg<sup>2+</sup> lane (-) and a 1-min time point after the addition of 10 mM Mg<sup>2+</sup> (+) are shown.

and a double mutant,  $\alpha$ C24g:G41c (Fig. 3F). As with the genomic mutants, only the wild-type sequence and the double mutant cleaved to an appreciable extent (86% and 72% cleavage, respectively; Fig. 4B). Kinetic studies revealed that the rate constants for cleavage of the single mutants  $\alpha$ C24g and  $\alpha$ G41c decreased relative to wild-type (24,000-fold and 530-fold reductions, respectively; Table 2). The  $\alpha$ C24g:G41c double mutant again restored activity and was found to cleave as fast or faster than the wild-type PEX1 ribozyme (40 min<sup>-1</sup> versus 31 min<sup>-1</sup>). These results provided evidence for base pairing between  $\alpha$ C24 and  $\alpha$ G41 in the antigenomic ribozyme.

### The top base pair of P1.1

The other base pair of the genomic P1.1 duplex,  $\gamma$ C22–G38, stacks below the  $\gamma$ G1•U37 wobble pair at the base of the P1 duplex (Fig. 2). The  $\gamma$ C22–G38 base pair forms the bottom of what can be viewed as the active-site pocket. Additionally, this base pair stacks on top of the P1.1 base pair described in the previous section. Two different sets of mutations were constructed for the  $\gamma$ C22–G38 base pair (Fig. 3A,B). The first set of mutations changed the C-G base pair to a G•G ( $\gamma$ C22g) and C•C ( $\gamma$ G38c) mismatch and to a G-C pair ( $\gamma$ C22g:G38c) (Fig. 3A). The two mismatch mutations reduced cleavage activity compared with the wild-type genomic ribozyme (Fig. 4A); the rate constant for cleavage of  $\gamma$ C22g was down approximately 1,900-fold, while cleavage of  $\gamma$ G38c was down about 900-fold (Table 1). The double mutant,  $\gamma$ C22g:G38c, though still 50-fold less active than wild-type, was significantly more active than either of the single mutants. The same mutations were tested at the predicted equivalent pair ( $\alpha$ C25–G40) of P1.1 in the antigenomic ribozyme:  $\alpha$ C25g (G•G mismatch),  $\alpha$ G40c (C•C mismatch), and  $\alpha$ C25g:G40c (restores base pairing potential) (Fig. 3D). Very similar results were found with these mutations (Fig. 4B). When the kinetics of cleavage were measured, the single mutations both slowed cleavage activity (7,700-fold in the case of  $\alpha$ C25g, 1,100-fold for  $\alpha$ G40c), whereas the double mutation ( $\alpha$ C25g:G40c) restored cleavage activity to nearly wild-type level (only a sevenfold reduction) (Table 2). This provided evidence that base pairing between these 2 nt is also required for cleavage activity in the antigenomic ribozyme.

A second set of mutations at  $\gamma$ C22–G38 were made that would maintain the pyrimidine:purine orientation at this position and would also allow us to test whether a noncanonical pyrimidine–purine pair could substitute for the C-G pair at this position. In the genomic ribozyme, two single mutants,  $\gamma$ C22u and  $\gamma$ G38a, and a double mutant,  $\gamma$ C22u:G38a, were made. The  $\gamma$ C22u mutant was predicted to create a U•G wobble pair at this position,  $\gamma$ G38a created a potential C•A mismatch, and  $\gamma$ C22u:G38a would restore canonical base pairing

potential to this position (Fig. 3B). As with the single mutants above that created potential mismatches,  $\gamma$ G38a caused a reduction in cleavage activity as compared to TGR-1 (Fig. 4A). In this case, the reduction was approximately 4,100-fold (Table 1). However, the  $\gamma$ C22u single mutant showed significant cleavage activity, and the cleavage rate constant was only 19-fold down compared to TGR-1. These data suggest that a U•G wobble pair could fulfill the pairing requirements at this position, but a C•A mismatch could not. The  $\gamma$ C22u:G38a double mutant cleaved with a rate constant similar to TGR-1 (only a sixfold reduction). Equivalent mutations to those described above were made in the antigenomic ribozyme. They were  $\alpha$ C25u (U•G wobble pair),  $\alpha$ G40a (C•A mismatch), and  $\alpha$ C25u:G40a (U-A canonical base pair) (Fig. 3E). Results were consistent with those found for the genomic ribozyme (Fig. 4B). The  $\alpha$ G40a cleavage rate constant was down 1,600-fold compared to wild-type,  $\alpha$ C25u was down 84-fold, and the double mutant ( $\alpha$ C25u:G40a) was essentially wild-type (less than a twofold decrease) (Table 2). Together, these data provide evidence for a rather flexible base pairing requirement for the  $\gamma$ C22–G38 and  $\alpha$ C25–G40 base pair in the genomic and antigenomic ribozymes, respectively. The wild-type C-G pair could be flipped to a G-C or replaced with either a U-A or a U•G pair with only a slight loss of activity. On the other hand, several mismatches (C•C, G•G and A•C) did not support cleavage activity at this position.

### Denaturants do not enhance activity of the P1.1 mutants

Many precursor sequences containing either the genomic or antigenomic HDV ribozyme cleave faster when moderate concentrations of urea or other denaturants are included in the reactions (Rosenstein & Been, 1990; Perrotta & Been, 1991; Smith & Dinter-Gottlieb, 1991). Enhancement of ribozyme activity by denaturants can indicate a tendency for the precursor RNA to misfold into a meta-stable form (Been & Wickham, 1997; Perrotta & Been, 1998; Treiber et al., 1998). While the addition of urea does not enhance cleavage activity of the wild-type precursors used in this study (Wadkins & Been, 1997; Perrotta & Been, 1998), testing the effect of urea on the variants may reveal whether mutations that slowed cleavage did so by interfering with a folding pathway or by increasing the stability of misfolded structures. The effect of urea was tested with all of the genomic variants and some of the antigenomic variants, and the effect was always to further slow cleavage with either no effect on or a decrease in the overall extent of cleavage (Table 1). These results, though not definitive, would argue against the likelihood that mutations in P1.1 only inhibited the reaction by increasing the accumulation of meta-stable misfolded structures.

## DISCUSSION

The functional importance of base pairing in the P1.1 duplex to cleavage activity was demonstrated by mutagenesis of genomic and antigenomic HDV ribozymes. Requirements for base pairing in P1, P2, P3, and P4 had already been established by similar approaches for both ribozymes (Been & Wickham, 1997). In those cases there were differences between genomic and antigenomic sequences that resulted in examples of base pair covariation and provided the initial evidence for the duplex elements (Perrotta & Been, 1991; Rosenstein & Been, 1991). No such covariation occurs with the sequences that form P1.1 in the antigenomic and genomic sequences. Thus, the results from mutagenesis that support a P1.1 base pairing requirement for cleavage activity, although anticipated from the crystal structure, are meaningful. They confirm a structure–function relationship for a previously untested structural feature identified in the crystallized postcleavage form of the ribozyme, and they provide additional evidence for proposing closely related structures for the genomic and antigenomic ribozymes.

The genomic and antigenomic ribozymes did not respond in exactly the same way to some of the changes in P1.1. Although these data suggest that other canonical base pairs can substitute for the C-G pairs, there was a clear preference for the wild-type pairing at both positions in the genomic ribozyme. The difference is largest in the bottom base pair ( $\gamma$ C21–G39), where flipping the pair slowed cleavage 84-fold ( $\gamma$ C21g:G39c; Table 1). In contrast, the antigenomic variant with the bottom base pair flipped showed no decrease in activity ( $\alpha$ C24g:G41c; Table 2). There is a possible structural basis for this disparity because of sequence differences in the two ribozymes: the antigenomic ribozyme does not contain a sequence equivalent to  $\gamma$ C41–A42–A43 ( $\gamma$ CAA) in J1.1/4. In fact, J1.1/4 may not exist in the antigenomic ribozyme as P1.1 may stack directly on a G•G pair ( $\alpha$ G42•G75) at the end of P4 (Been & Perrotta, 1995; Wickham et al., 1997). In the genomic ribozyme, there is a large propeller twist of the  $\gamma$ C21–G39 pair (Fig. 2), and the minor groove side of  $\gamma$ C21 participates in two additional hydrogen bonds through its O2 and O2' positions to the base of  $\gamma$ A42. In the antigenomic ribozyme, the equivalent nucleotide,  $\alpha$ C24, would presumably not participate in similar minor groove hydrogen bonding as there is no obvious equivalent to  $\gamma$ A42. There is evidence, however, that even in the genomic ribozyme, the contact between  $\gamma$ A42 and the minor groove side of  $\gamma$ C21 is not essential, as the  $\gamma$ CAA sequence can be deleted from the genomic ribozyme without loss of activity (Wadkins & Been, 1997). One possible explanation for the different responses to this base-pair change in P1.1 is that even if the approximate hydrogen bonding pattern in the minor groove could be maintained after flipping the  $\gamma$ C21–G39 base

pair (with the N3 of G replacing the O2 of C as an H-bond acceptor), that minor groove contact would slightly change the position of the altered P1.1 and affect activity. In contrast, for the antigenomic ribozyme, if P1.1 stacks on  $\alpha$ G42•G75 at the end of P4 (Been & Perrotta, 1995; Wickham et al., 1997) without making additional H-bonds, it may be less sensitive to base-pair alterations.

Several base-pairing schemes were tested for the position at the top of P1.1. The evidence suggested that the preference at this position is both for a stable base pair and for an orientation that maintains the purine at position  $\gamma$ 38 ( $\alpha$ 40). In addition to a C-G flip, a potential U-A pairing and U•G wobble were tested at this position. The latter combinations have the potential to maintain the purine–purine cross-strand stacking interaction between G1 and position  $\gamma$ 38 (Fig. 2). In both ribozymes, the U-A substitution, which would maintain the pyrimidine–purine orientation of the wild-type base pair, was marginally (three- to eightfold) more active than flipping the C-G pair (Tables 1 and 2). Of the four mismatches that were tested at this position (C•C, G•G, U•G, and C•A), U•G was the most active. While U•G was 40-fold less active than the U-A pair in the antigenomic, it was only threefold less active than the U-A in the genomic. In contrast, the C•A mismatch at this position was significantly less active than the U•G in both ribozymes.

In the ribozyme precursor, the top base pair of P1.1 effectively blocks the possibility of continuing P1 in the 5' direction. It would appear, from inspection of the earlier secondary structures, that the pyrimidine at the –1 position could pair with  $\gamma$ G38 ( $\alpha$ G40), extending P1 by an additional base pair and competing with the top base pair in P1.1. In some models for the secondary structure of the HDV ribozyme precursors, the nucleotide 5' to the cleavage site ( $\gamma$ U-1 and  $\alpha$ C-1) was proposed to pair with  $\gamma$ G38 ( $\alpha$ G40) of P1.1. This proposed base pair is somewhat unappealing from a mechanistic standpoint in that it would place the scissile phosphate within a duplex, and it was also inconsistent with the lack of evidence for strong sequence specificity at the –1 position (Perrotta & Been, 1992, 1996). This lack of sequence specificity has made it difficult to identify a potential binding surface for the sequence 5' to the cleavage site. The evidence presented in this article, although not ruling out a transient pairing between the –1 base (U or C) and  $\gamma$ G38 ( $\alpha$ G40), strongly suggests that such pairing, if it occurs at all during the reaction cycle, is not essential for the cleavage reaction.

The results presented here support an essential role for P1.1 in cleavage activity of both of the HDV ribozymes. Accordingly, the secondary structure model of the antigenomic ribozyme was revised to include P1.1. The mutagenesis data are consistent with the crystal structure and support the idea that, despite their proximity to the active site, the bases forming P1.1 probably

do not provide essential functional groups necessary for catalysis but rather fulfill primarily a structural role in both defining an active-site pocket and bringing essential active-site components together near the scissile phosphate.

## MATERIALS AND METHODS

### Enzymes and chemicals

T7 RNA polymerase was purified by M. Puttaraju from an overexpressing clone provided by W. Studier (Davanloo et al., 1984). Modified T7 DNA polymerase (Sequenase) was purchased from U.S. Biochemical (Cleveland). Other supplies were purchased from commercial suppliers. Oligonucleotides were synthesized on an Applied Biosystems DNA synthesizer (Department of Botany, Duke University, Durham, North Carolina).

### Plasmid construction

The version of the genomic ribozyme sequence used in this study (TGR-1) has been described previously (Wadkins & Been, 1997). Mutants were generated by oligonucleotide-directed mutagenesis using a uracil-containing, single-stranded form of the plasmid as the template (Kunkel et al., 1987; Vieira & Messing, 1987). Plasmids with mutations were identified by sequencing mini-prep DNA. Following a second round of transformation, plasmid DNA was prepared from overnight cultures and purified by CsCl equilibrium density ultracentrifugation in the presence of ethidium bromide (Maniatis et al., 1982). All purified plasmid DNA was again sequenced before use as templates in transcriptions. The version of the antigenomic ribozyme sequence used in this study (PEX1) has also been described previously (Perrotta & Been, 1998). Base changes to this initial sequence were made as described above (Kunkel et al., 1987; Vieira & Messing, 1987).

### Transcriptions

Mini-prep and plasmid DNA were linearized by digestion with *Bam*HI (genomic constructs) or *Ban*I (antigenomic constructs), extracted with phenol and chloroform, ethanol precipitated, and transcribed in 0.05 mL reactions containing 40 mM Tris-HCl (pH 7.5), 15 mM MgCl<sub>2</sub>, 5 mM dithiothreitol, 2 mM spermidine, ribonucleoside triphosphates at 1 mM each, 0.04 mCi [ $\alpha$ -<sup>32</sup>P]GTP, 2.5–5  $\mu$ g linear plasmid DNA and 300 U T7 RNA polymerase. Incubation was for 60 min at 37 °C, EDTA was added to 50 mM, formamide to 50% (v/v), and the RNA was fractionated by electrophoresis on a 6% (w/v) polyacrylamide gel containing 7 M urea. RNA was located by autoradiography, excised, eluted, and recovered by ethanol precipitation. RNAs were stored in 0.1 mM EDTA at –20 °C.

### Cleavage assays

Radiolabeled precursor RNA was heated at 95 °C for 1 min in 0.1 mM EDTA. The RNA was then preincubated at 37 °C for 10 min in the cleavage cocktail minus Mg<sup>2+</sup>, and the cleavage reactions were initiated by addition of MgCl<sub>2</sub> (37 °C).

Final conditions for the genomic constructs were 40 mM Tris-HCl (pH 8.0), 1 mM EDTA, 11 mM MgCl<sub>2</sub> and 5–50 nM RNA. Final conditions for the antigenomic constructs were 40 mM Tris-HCl (pH 7.5), 1 mM EDTA, 0.5 mM spermidine (included during the preincubation), 11 mM MgCl<sub>2</sub> and 5–50 nM RNA. The kinetics of cleavage were followed by removing aliquots at specified times and mixing them with formamide-dye mix containing EDTA to quench the reaction. The precursor and product were separated by gel electrophoresis under denaturing conditions (6% polyacrylamide gels containing 7 M urea, 0.05 M Tris-borate (pH 8.3), 0.5 mM EDTA). The relative amounts of precursor and 3'-cleavage product were quantified by analysis in a phosphorimager (Molecular Dynamics). After correcting the counts for background, the fraction cleaved (F) was calculated as (counts<sub>product</sub>)/(counts<sub>precursor</sub> + counts<sub>product</sub>). The 3' product contained 91–92% of the label for the antigenomic precursors used in this study and 97% of the label for the genomic precursors. The 5' product migrates off these gels and was not included directly in the analysis. Data were corrected for loss of the 5' product radioactivity in cases where effects of the loss were found to be significant on values obtained for the rate constants. The first order rate constant (k) and endpoint (F<sub>∞</sub>) were obtained by fitting the data to  $F = F_{\infty} \times (1 - e^{-kt})$ , where F is the fraction cleaved at time t. The endpoints seen in reactions with purified precursors most likely did not reflect a true equilibrium between the cleaved and uncleaved forms, as the extent of cleavage can vary for different methods of preparation of the precursor. In addition, the extent of cleavage seen with purified precursor was routinely different than the extent of cleavage observed during transcription. More likely, the endpoint represents a combination of contaminating species that comigrate with the precursor during gel purification and noncleaving conformers of the ribozymes. For some of the precursors, the reaction was complete after 1 min, and the earliest time points were taken at 4 or 5 s. Thus, although reproducibility was good, we may have underestimated the fastest reactions. For the precursor RNAs that cleaved more slowly, reproducibility was usually within  $\pm 10\%$ . Kinetic data reported for the reactions without urea were the average of at least three independent determinations from two independent preparations of the RNA. Kinetic data obtained for the genomic constructs in urea were the average of either two determinations or the result of a single determination when the data were essentially identical to the result without urea.

## ACKNOWLEDGMENTS

We thank I-h. Shih for comments on the manuscript. This work was supported by a grant from the National Institutes of Health to M.D.B (GM47233). J.A.D. receives support from the Howard Hughes Medical Institute.

Received February 2, 1999; returned for revision February 17, 1999; revised manuscript received March, 10, 1999

## REFERENCES

- Been MD, Perrotta AT. 1995. Optimal self-cleavage activity of the hepatitis delta virus RNA is dependent on a homopurine base pair in the ribozyme core. *RNA* 1:1061–1070.

- Been MD, Wickham GS. 1997. The self-cleaving ribozymes of Hepatitis Delta Virus. *Eur J Biochem* 247:741–753.
- Davanloo P, Rosenberg AH, Dunn JJ, Studier FW. 1984. Cloning and expression of the gene for bacteriophage T7 RNA polymerase. *Proc Natl Acad Sci USA* 81:2035–2039.
- Ferré-D'Amaré AR, Zhou K, Doudna JA. 1998. Crystal structure of a hepatitis delta virus ribozyme. *Nature* 395:567–574.
- Jeng K-S, Daniel A, Lai MMC. 1996. A pseudoknot ribozyme structure is active in vivo and required for hepatitis delta virus RNA replication. *J Virol* 70:2403–2410.
- Kawakami J, Kumar PKR, Suh Y-A, Nishikawa F, Kawakami K, Taira K, Ohtsuka E, Nishikawa S. 1993. Identification of important bases in a single-stranded region (SSrC) of the hepatitis delta ( $\delta$ ) virus ribozyme. *Eur J Biochem* 217:29–36.
- Kos A, Dijkema R, Arnberg AC, van der Meide PH, Schellekens H. 1986. The hepatitis delta ( $\delta$ ) virus possesses a circular RNA. *Nature* 323:558–560.
- Kumar PKR, Suh Y-A, Taira K, Nishikawa S. 1993. Point and compensation mutations to evaluate essential stem structures of genomic HDV ribozyme. *FASEB J* 7:124–129.
- Kumar PKR, Taira K, Nishikawa S. 1994. Chemical probing studies of variants of the genomic hepatitis delta virus ribozyme by primer extension analysis. *Biochemistry* 33:583–592.
- Kunkel TA, Roberts JD, Zakour RA. 1987. Rapid and efficient site-specific mutagenesis without phenotypic selection. *Methods Enzymol* 154:367–382.
- Kuo MY-P, Sharmeen L, Dinter-Gottlieb G, Taylor J. 1988. Characterization of self-cleaving RNA sequences on the genome and antigenome of human hepatitis delta virus. *J Virol* 62:4439–4444.
- Lai MMC. 1995. The molecular biology of hepatitis delta virus. *Annu Rev Biochem* 64:259–286.
- MacNaughton TB, Wang Y-J, Lai MMC. 1993. Replication of hepatitis delta virus RNA: Effect of mutations of the autocatalytic cleavage sites. *J Virol* 67:2228–2234.
- Maniatis T, Fritsch EF, Sambrook J. 1982. *Molecular cloning: A laboratory manual*. Cold Spring Harbor, New York: Cold Spring Harbor Laboratory Press.
- Perrotta AT, Been MD. 1990. The self-cleaving domain from the genomic RNA of hepatitis delta virus: Sequence requirements and the effects of denaturant. *Nucleic Acids Res* 18:6821–6827.
- Perrotta AT, Been MD. 1991. A pseudoknot-like structure required for efficient self-cleavage of hepatitis delta virus RNA. *Nature* 350:434–436.
- Perrotta AT, Been MD. 1992. Cleavage of oligoribonucleotides by a ribozyme derived from the hepatitis  $\delta$  virus RNA sequence. *Biochemistry* 31:16–21.
- Perrotta AT, Been MD. 1996. Core sequences and a cleavage site wobble pair required for HDV antigenomic ribozyme self-cleavage. *Nucleic Acids Res* 24:1314–1321.
- Perrotta AT, Been MD. 1998. A toggle duplex in Hepatitis Delta Virus self-cleaving RNA that stabilizes an inactive and a salt-dependent pro-active ribozyme conformation. *J Mol Biol* 279:361–373.
- Pleij CWA. 1990. Pseudoknots: A new motif in the RNA game. *Trends Biochem Sci* 15:143–147.
- Pleij CWA, Rietveld K, Bosch L. 1985. A new principle of RNA folding based on pseudoknotting. *Nucleic Acids Res* 13:1717–1731.
- Pley HW, Flaherty KM, McKay DB. 1994. Three-dimensional structure of a hammerhead ribozyme. *Nature* 372: 68–74.
- Rizzetto M. 1983. The delta agent. *Hepatology* 3:729–737.
- Rosenstein SP, Been MD. 1990. Self-cleavage of hepatitis delta virus genomic strand RNA is enhanced under partially denaturing conditions. *Biochemistry* 29:8011–8016.
- Rosenstein SP, Been MD. 1991. Evidence that genomic and antigenomic RNA self-cleaving elements from hepatitis delta virus have similar secondary structures. *Nucleic Acids Res* 19:5409–5416.
- Rosenstein SR, Been MD. 1996. Hepatitis delta virus ribozymes fold to generate a solvent-inaccessible core with essential nucleotides near the cleavage-site phosphate. *Biochemistry* 35:11403–11413.
- Scott WG, Finch JT, Klug A. 1995. The crystal structure of an all-RNA hammerhead ribozyme: A proposed mechanism for RNA catalytic cleavage. *Cell* 81:991–1002.
- Sharmeen L, Kuo MY-P, Dinter-Gottlieb G, Taylor J. 1988. Antigenomic RNA of human hepatitis delta virus can undergo self-cleavage. *J Virol* 62:2674–2679.
- Smith JB, Dinter-Gottlieb G. 1991. Antigenomic hepatitis delta virus ribozymes self-cleave in 18 M formamide. *Nucleic Acids Res* 19:1285–1289.
- Symons RH. 1992. Small catalytic RNAs. *Ann Rev Biochem* 61:641–671.
- Tanner NK, Schaff S, Thill G, Petit-Koskas E, Crain-Denoyelle A-M, Westhof E. 1994. A three-dimensional model of hepatitis delta virus ribozyme based on biochemical and mutational analyses. *Curr Biol* 4:488–497.
- Thill G, Vasseur M, Tanner NK. 1993. Structural and sequence elements required for the self-cleaving activity of the hepatitis delta virus ribozyme. *Biochemistry* 32:4254–4262.
- Treiber DK, Rook MS, Zarrinkar PP, Williamson JR. 1998. Kinetic intermediates trapped by native interactions in RNA folding. *Science* 279:1943–1946.
- Vieira J, Messing J. 1987. Production of single-stranded plasmid DNA. *Methods Enzymol* 153:3–11.
- Wadkins TS, Been MD. 1997. Core-associated non-duplex sequences distinguishing the genomic and antigenomic self-cleaving RNAs of hepatitis delta virus. *Nucleic Acids Res* 25:4085–4092.
- Wang K-S, Choo Q-L, Weiner AJ, Ou J-H, Najarian RC, Thayer RM, Mullenbach GT, Denniston KJ, Gerin JL, Houghton M. 1986. Structure, sequence and expression of the hepatitis delta ( $\delta$ ) viral genome. *Nature* 323:508–514.
- Wickham GS, Shih I-h, Been MD. 1997. Molecular modeling of a G•G basepair in the antigenomic HDV ribozyme. *Nucleic Acids Symp Ser* 36:99–101.
- Wu H-N, Lin Y-J, Lin F-P, Makino S, Chang M-F, Lai MMC. 1989. Human hepatitis  $\delta$  virus RNA subfragments contain an autocleavage activity. *Proc Natl Acad Sci USA* 86:1831–1835.